# Examination of New CERES Data for Evidence of Tropical Iris Feedback

LIN H. CHAMBERS, BING LIN, AND DAVID F. YOUNG

*Radiation and Aerosols Branch, NASA Langley Research Center, Hampton, Virginia*

(Manuscript received 18 April 2002, in final form 7 July 2002)

ABSTRACT

New data products from the Clouds and the Earth's Radiant Energy System (CERES) instrument on the Tropical Rainfall Measuring Mission Satellite have been examined in the context of the recently proposed adaptive tropical infrared Iris hypothesis. The CERES Single Scanner Footprint data products combine radiative fluxes with cloud properties obtained from a co-orbiting imaging instrument. This enables the use of cloud property–based definitions of the various regions in the simple Iris climate model. Regardless of definition, the radiative properties are found to be different from those assigned in the original Iris hypothesis. As a result, the strength of the feedback effect is reduced by a factor of 10 or more. Contrary to the initial Iris hypothesis, most of the definitions tested in this paper result in a small positive feedback. Thus, the existence of an effective infrared iris to counter greenhouse warming is not supported by the CERES data.

## 1. Introduction

New data products from the Clouds and the Earth's Radiant Energy System (CERES; Wielicki et al. 1996) instrument were recently released. The Single Scanner Footprint (SSF) data product combines radiation budget data from CERES with cloud property retrievals from an imager on the same platform to provide a vastly improved characterization of the state of the atmosphere. In addition, the SSF incorporates new CERES angular distribution models (ADMs; Loeb et al. 2003) based on improved scene identification to obtain more accurate top-of-the-atmosphere fluxes from the satellite-measured radiances. Together these advances allow the study of radiative fluxes for specific cloud types with unprecedented accuracy. With prior datasets such as the Earth Radiation Budget Experiment (ERBE; Barkstrom et al. 1989), only monthly mean fluxes could be relied on for their accuracy. SSF data products are now available using CERES and the Visible and Infrared Scanner (VIRS) on the Tropical Rainfall Measuring Mission (TRMM) satellite.

CERES TRMM SSF data have been used to explore the Iris hypothesis recently proposed by Lindzen et al. (2001, hereafter LCH). This hypothesis is based upon the observation, from geostationary data, that high cloud amount decreases with SST in the tropical west Pacific (TWP) and that there is a sharp boundary between dry and moist portions of the upper troposphere. The moist portions are assumed to result from convection and cirrus outflow, while the dry portions are associated with broad downwelling areas. LCH used these observations to develop a 3.5-box climate model consisting of the extratropics and the dry and moist Tropics. LCH further divided the moist Tropics into a cloudy-moist region containing upper-level cirrus cloud and a clear-moist region without this high cirrus. LCH then assigned radiative properties, constrained by ERBE global and tropical mean values, to the various parts of the model. They concluded that a strong negative feedback occurred: increasing SST led to decreased cirrus cloudiness, more thermal infrared (IR) radiation escaping to space, and thus less greenhouse trapping by clouds.

The Iris hypothesis has been examined by several other researchers. Hartmann and Michelsen (2002) examined the variation of high cloud amount with SST and concluded that it responds more to changes in subtropical clouds than to changes in tropical convection. Fu et al. (2002) used a radiative transfer model that showed that the feedback due to the Iris effect was overestimated in LCH. Lin et al. (2002) used CERES ERBE-like data and also concluded that the LCH radiative properties incorrectly lead to a strong negative feedback.

In the current work, the radiative properties of the 3.5-box climate model are reexamined using measured radiation fluxes from the CERES SSF products. The SSF differs from the ERBE-like data product in that it includes retrieved cloud properties and uses improved ADMs based on the enhanced scene identification. Each box in the model can be identified according to param-

*Corresponding author address:* Lin H. Chambers, Radiation and Aerosols Branch, NASA Langley Research Center, MS 420, Hampton, VA 23681-2199.
E-mail: l.h.chambers@larc.nasa.gov

eters on the SSF. The dry region, assumed by LCH to cover half the Tropics, is assigned the radiative properties of the 50% of CERES footprints in the tropical maritime area that have the warmest longwave fluxes. This corresponds to IR emission from the lowest levels of the atmosphere as occurs when the atmosphere contains little water vapor. The definition of the cloudy-moist and clear-moist regions is explored in this study, using retrieved cloud properties to better identify these regions.

Section 2 gives a brief description of the CERES instrument and operation. Section 3 details the data analysis performed in this study. Section 4 presents the improved radiative properties and compares them to those used by LCH. Section 5 examines the feedback effect using the new radiative properties. Section 6 gives a summary and conclusions.

## 2. The CERES instrument

The CERES instrument is a biaxial scanning radiometer (Wielicki et al. 1996). On the TRMM satellite, CERES operated in a quasiperiodic cycle of two days in fixed azimuth plane scan (FAPS) mode and one day in rotating azimuth plane scan (RAPS) mode, with an occasional day of along-track scanning. FAPS mode is basically a cross-track scanning mode and obtains maximum geographic coverage over the orbital swath. RAPS mode scans in azimuth in order to obtain information on the anisotropy of radiation in the full hemisphere. The TRMM satellite is a precessing spacecraft with an orbital inclination of about 35°. It samples all local times over a 46-day period.

CERES measures radiative energy in three broad channels: the shortwave (SW) channel measures reflected solar radiation, the window (WN) channel measures thermal radiation between 8.10 and 11.79 $\mu$m, and the total (TOT) channel measures the total energy leaving the earth at all wavelengths, limited only by the spectral characteristics of the radiometer ($0.3 \rightarrow 100$ $\mu$m; Priestley et al. 2000). The longwave (LW) radiation is obtained by subtraction: LW = TOT − SW.

CERES is primarily a climate instrument, so great attention has been paid to its calibration. As a result, the CERES measurements have been both stable and accurate over the lifetime of the instrument. Uncertainties in measured radiances are generally below the 0.5% level (Priestley et al. 2000). The errors in the instantaneous estimated fluxes of SW (13 W m$^{-2}$) and LW (4.3 W m$^{-2}$) radiation are mainly due to errors in the application of the angular distribution models (Wielicki et al. 1995; Loeb et al. 2003), which result from errors in the scene identification (Chambers et al. 2001).

## 3. Data analysis

A CERES SSF data product contains approximately 130 parameters describing each CERES measurement. These include time, position, and viewing angles, surface information, filtered and unfiltered radiances, radiative fluxes at the surface and top of atmosphere, and a variety of parameters describing the clear and cloudy portions of the footprint. The latter are obtained from imager (VIRS) information and from ancillary inputs such as numerical weather prediction models (Minnis et al. 1999; Loeb et al. 2003). The analysis includes a sophisticated multispectral cloud mask with multiple layers of tests and a tailored approach to nighttime cloud detection (Minnis et al. 1998). For cloudy VIRS pixels, the visible infrared solar-infrared technique (VIST; Minnis et al. 2002) is applied to retrieve cloud properties through an iterative technique that matches measured spectral radiances to computed spectral radiances for a range of cloud microphysical properties and cloud temperature, $T_c$. The nominal 2-km VIRS pixel–derived properties are then convolved using the CERES scanner point spread function to obtain cloud properties within the CERES footprint (the half-power size of a CERES TRMM footprint at nadir is nominally 10 km; Green and Wielicki 1995). The SSF contains information on up to two cloud layers, which are separated by at least 50 hPa, and which are convolved separately. Currently these layers are distinct, with no overlap properties identified.

For this analysis, since radiative fluxes are only available at the CERES footprint scale, the properties of the two cloud layers are combined using area weighting to obtain footprint-mean cloud properties. Since detection of upper-level cirrus is of particular interest here, the properties of the upper layer alone are also examined. If the upper cloud layer fills more than half the CERES footprint, the tests described in section 4b are also applied to the properties of the upper layer only. (Note that if only a single cloud layer can be identified, its properties are assigned to the ''lower'' layer, regardless of the actual cloud height.)

The SSF is a level-2 data product, so footprints with problems have already been flagged as such, and are not used. Each footprint is also checked for default values of key parameters, such as the WN radiance, SW and LW flux, and clear area fraction. If these parameters are not defined, the footprint is not considered in the analysis. Because the VIRS viewing angle is restricted to a maximum of 48°, some CERES footprints are only partially covered by VIRS measurements—or not covered at all. Thus, footprints are also screened for high imager coverage (>60%) and minimal extrapolation of cloud properties (<30%) to ensure that the cloud properties used for the footprint are representative. Two sunglint tests are applied to screen out footprints where either CERES or the VIRS imager is in a glint condition. Cloud property retrieval errors are greater in the presence of sunglint. Application of this set of screening criteria leaves more than half a million regionally distributed footprints per day to be analyzed.

CERES TRMM SSF data are available for the period 1 January–31 August 1998. This includes the peak and decay of the strong 1997/98 El Niño. Short periods of data are available after this, but are not included in this study because of the precessing orbit. Along-track days are also not included, due to poor spatial sampling. To prevent temporal sampling biases, the TRMM data are analyzed in 46-day intervals to get complete sampling of the radiative properties over the full range of local times. This is necessary to get a correct insolation-weighted albedo. For a given latitude zone, $x_j$, and 46-day period, $t_k$, the insolation-weighted albedo for a given class of $M$-type footprints, $\alpha_M$, is given by

$$\alpha_M(x_j, t_k) = \frac{\sum_{i=1}^{N} \alpha_M(\theta_{0i}, x_j, t_k) S_f(\theta_{0i}, x_j, t_k) \cos\theta_{0i} F_M(\theta_{0i}, x_j, t_k)}{\sum_{i=1}^{N} S_f(\theta_{0i}, x_j, t_k) \cos\theta_{0i} F_M(\theta_{0i}, x_j, t_k)}, \quad (1)$$

where $S_f(\theta_{0i}, x_j, t_k)$ is the theoretical fraction of time that the sun is in solar zenith bin $\theta_{0i}$ for latitude zone $j$ and precession cycle $k$, and $F_M(\theta_{0i}, x_j, t_k)$ is the fraction of footprints that meet a particular criterion, $M$ (such as tropical dry, deep convection, or cirrus, as identified with parameters from the SSF). The $\alpha_M(\theta_{0i}, x_j, t_k)$ is the mean albedo of the $M$-type footprints. The instantaneous footprint albedo is first corrected to the mean Earth–Sun distance, and also adjusted to the center of the solar zenith angle bin by the ratio $\cos(\theta_c)/\cos(\theta_0)$, where $\theta_0$ and $\theta_c$ are the footprint solar zenith angle and the angle at the bin center, respectively.

The zonal albedo is further reduced to a spatially averaged value as follows:

$$\alpha_M(t_k) = \frac{\sum_{j=1}^{J} A(x_j) S_p(x_j, t_k) \sum_{i=1}^{N} \alpha_M(\theta_{0i}, x_j, t_k) S_f(\theta_{0i}, x_j, t_k) \cos\theta_{0i} F_M(\theta_{0i}, x_j, t_k)}{\sum_{j=1}^{J} A(x_j) S_p(x_j, t_k) \sum_{i=1}^{N} S_f(\theta_{0i}, x_j, t_k) \cos\theta_{0i} F_M(\theta_{0i}, x_j, t_k)}. \quad (2)$$

Here, $A(x_j) = \cos(\text{lat}_j)$ is the area weighting for each zonal band, and $S_p$ is the total insolation in a latitude band for a given 46-day period. The final albedo for the domain over the whole period is the average of the values from each of the five 46-day periods:

$$\overline{\alpha_M} = \frac{1}{5} \sum_{k=1}^{5} \alpha_M(t_k). \quad (3)$$

The LW flux is obtained in a similar, but simpler fashion, since neither the Sun–Earth distance correction nor the weighting by solar zenith angle are required. This does not imply a lack of diurnal variation in the LW flux, only that the LW weighting does not depend on the time of day. The diurnal variation of the LW flux is measured during the precession cycle and included in the average. Here

$$\text{LW}_M(x_j, t_k) = \left( \sum_{l=1}^{L_{\text{fp}}} \text{LW}_M^l \right) \Big/ L_{\text{fp}}, \quad (4)$$

where $\text{LW}_M^l$ is the outgoing LW flux for a CERES footprint meeting criterion $M$, and $L_{\text{fp}}$ is the total number of such footprints.

Given the near-radiative balance among the regions (see sections 4 and 5), correctly averaging the radiative properties is crucial. If the solar zenith weighting is (incorrectly) applied to the LW flux, the resulting mean LW flux shifts very slightly. However, this shift is sufficient to tip several of the cases considered from a positive to a negative (but still very small) feedback. If the weightings are not correctly applied in obtaining the average albedo, energy is not conserved and the results will be incorrect.

The radiative properties of a particular $M$-type footprint are found to be very stable from one precession cycle to the next, suggesting that the results are in fact representative of that cloud–atmosphere type; and not responding to a seasonal or El Niño signal.

Three tropical ocean regions between 30°S and 30°N latitude are considered: the tropical west Pacific (TWP) between 130° and 190°E (this corresponds to the region studied by LCH); the east Pacific between 200° and 280°E; and the entire tropical ocean within 30°S–30°N. When calculating the radiative properties, each region was broken up into 10° latitude zones. For the land mask, SSF footprints are screened by surface scene type for complete coverage by water.

TABLE 1. Properties for the 3.5-box climate model.

| Region | Definition | Frequency of occurrence | SW albedo | OLR (W m$^{-2}$) | Net flux (W m$^{-2}$) | Cloud fraction |
|---|---|---|---|---|---|---|
| Dry | Highest 50% of LW | 0.50* | 0.14 | 292 | 51.4 | 0.23 |
| Moist | Lowest 50% of LW | 0.50 | 0.32 | 231 | 42.4 | 0.87 |
| Tropical ocean | | 1.0 | 0.23 | 262 | 46.9 | 0.55 |
| Dry | LCH values | 0.50* | 0.21 | 303 | 12.8 | 0.25 |
| Moist | LCH values | 0.50 | 0.28 | 208 | 84.3 | 0.58 |
| Tropical ocean | | 1.0 | 0.25 | 256 | 48.6 | 0.42 |

* By definition.

## 4. Radiative properties

### *a. The original 3.5-box model*

The Iris hypothesis of LCH relied on examination of the variation of cirrus cloud coverage with cloud-weighted SST over a large area. This was done using the 11- and 12-$\mu$m split window channels on Japan's Geostationary Meteorological Satellite, *GMS-5*. With this instrument, only limited information on the cloud properties could be obtained. Thus, LCH used the brightness temperature at 11 $\mu$m, $T_{11} < 260$ K, as an indicator of the cloudy-moist area of their simple 3.5-box climate model. Further, LCH used a subjective approach to select the radiative properties of each box in the climate model, subject to the constraint of matching ERBE (Barkstrom et al. 1989) global and tropical mean values. The LCH radiative properties have been subject to question from a radiative transfer model approach (Fu et al. 2002) and from analysis of CERES ERBE-like data (Lin et al. 2002). Both studies suggest that the LCH LW flux and SW albedo for the cloudy-moist portion of the model are too low, while the corresponding properties of the dry portion are too high.

Additional insight on the radiative properties of the various tropical regions can be obtained from the SSF data. The dry region, which LCH assume covers half the Tropics, is identified with those footprints having the highest 50% of outgoing LW flux [outgoing longwave radiation (OLR)] as done by Lin et al. (2002). This corresponds to OLR emitted from the lowest levels of the atmosphere, as occurs with very low upper-troposphere humidity. The moist region is then identified with the remaining 50% of footprints (lowest 50% of OLR). The radiative properties of these two regions, obtained from the CERES SSF measurements and from the LCH model, are summarized in Table 1. In agreement with Lin et al. (2002), who used the VIRS 10.8-$\mu$m brightness temperature and fluxes from the ERBE-like data product rather than SSF, we find higher (lower) LW flux and SW albedo in the moist (dry) region than the properties assigned by LCH. Also of interest are the measured cloud fractions in each region. The SSF finds 23% cloud cover in the dry region, compared to the LCH assumption of 25%. However, in the moist region the SSF finds 87% cloud cover, compared to the 58% assumed by LCH. This results in a tropical ocean cloud fraction in LCH that is substantially lower than that from CERES and other studies (Rossow et al. 1993).

### *b. Improved cloudy-moist definitions*

The use of a brightness temperature threshold to identify upper-level cirrus clouds is problematic. When the brightness temperature threshold is set very low, to remove all water clouds, it will also miss thinner cirrus clouds. When the threshold is too high, water clouds will be selected along with the cirrus clouds. Chou et al. (2002) indicated that $T_{11} < 260$ K was merely an index for the variation of the cloudy-moist region, and LCH actually used an area fraction about twice that of the $T_{11} < 260$ K region for the cloudy-moist box. The CERES SSF contains vastly improved information on cloud properties, including cloud temperature and cloud particle condensation phase (i.e., water or ice), using associated VIRS imager data. As a result, determination of cloud and radiative properties can be done in a much more objective way. With the SSF, retrieved cloud properties themselves can be examined to obtain a better identification of cirrus clouds. Two basic approaches are considered here: 1) $T_c$ tests find CERES footprints where the retrieved *cloud temperature* (accounting for the emissivity of thin clouds; Minnis et al. 1998) is suggestive of ice clouds; 2) cloud water/ice phase tests find CERES footprints in which the cloud is mostly or predominantly ice. These properties are used because they are obtained directly from the VIRS radiances.

Retrieval of cloud properties by remote sensing is subject to some difficulties. There are two kinds of errors related to high cloud detection: 1) missing high clouds entirely or 2) misidentifying high clouds as low- or midlevel clouds. Comparison to ground observer results shows no evidence that the CERES algorithm is missing anything more than isolated thin cirrus (0%–5% cloud fraction; Chambers et al. 2002, manuscript submitted to *Bull. Amer. Meteor. Soc.*), at least as long as the cirrus is thick enough to be visible. Initial validation studies of the CERES SSF cloud properties against cirrus-only cases from ground-based instruments show that the $T_c$ retrieval places cirrus clouds within 1 km of their actual height; while the phase retrieval is excellent for ice clouds (P. Minnis 2002, personal com-

munication). Thus, both kinds of errors related to cirrus cloud systems are small.

For multilayer cloud systems, that is, for cirrus over low- or midlevel water clouds, the retrieval is more complicated. Some thin cirrus over lower clouds will be missed in this analysis, resulting in retrieval of a water cloud that is somewhat too high and whose properties are somewhat affected by the intervening ice layer. This only occurs when the cirrus is thin, so that the radiative properties are close to those of the water cloud alone (which is why the cirrus is not detected). Some of these footprints may then improperly be placed in the clear-moist region, as opposed to the cloudy-moist region. The effects of this misclassification on the radiation fields of the cloudy-moist and clear-moist regions should not be large, as these footprints are dominated by the radiative properties of the water cloud.[1] Thus, some multilayer footprints will be lumped with single-layer water clouds in clear moist, and some with cirrus over water clouds in cloudy moist. As will be shown below, the net flux is not very sensitive to the details of the cloudy-moist definition, confirming that this source of error is not a major issue.

Using the CERES SSF, candidate improved criteria for identifying the cloudy-moist (cirrus covered) region can be tested. These include cloud temperature thresholds, $T_c < -15$°C and $T_c < -30$°C; and phase thresholds of phase $> 1.5$ (more than half of cloud in footprint is ice) and phase $> 1.9$ (cloud in footprint is predominantly ice). These properties are defined for the cloudy portion of a CERES footprint. Thus, a series of threshold cloud fractions is also imposed: $A_c > 0$, $>0.5$, $>0.95$, $>0.99$. The latter best corresponds to the LCH model, where the cloudy-moist region was assumed to be completely covered by cirrus. If the upper cloud layer covers more than half the CERES footprint, the same set of tests is also performed using only the properties of the upper cloud layer. This captures any occurrence of extensive and identifiable high cirrus cloud in the same footprint with identifiable low cloud.

Figure 1 summarizes the SW and LW radiative properties for the cloudy-moist region according to various definitions. CERES SSF results and the values used by LCH are shown. For both the $T_c$ and phase tests, there is a consistent trend in radiative properties as a function of the cloudy-moist area fraction found with the various tests. The cloudy-moist area coverage found with these definitions varies more than a factor of 3 from 0.09 to 0.30. The radiative properties change also, but relatively little (0.35–0.49 or ±17% for SW albedo, and 166–209 W m$^{-2}$ or ±11% for OLR). The water/ice phase tests result in a slightly darker cloudy-moist region than do the $T_c$ tests. This figure suggests that the main problem in LCH is the specification of a LW flux for the cloudy-moist region that is substantially lower than the CERES-derived values; while the LCH SW albedo is only slightly lower. As pointed out by Lin et al. (2002) and by Fu et al. (2002), the inconsistency of LW and SW radiative properties used by LCH enhanced the cooling effect of the cloud feedback in their results.

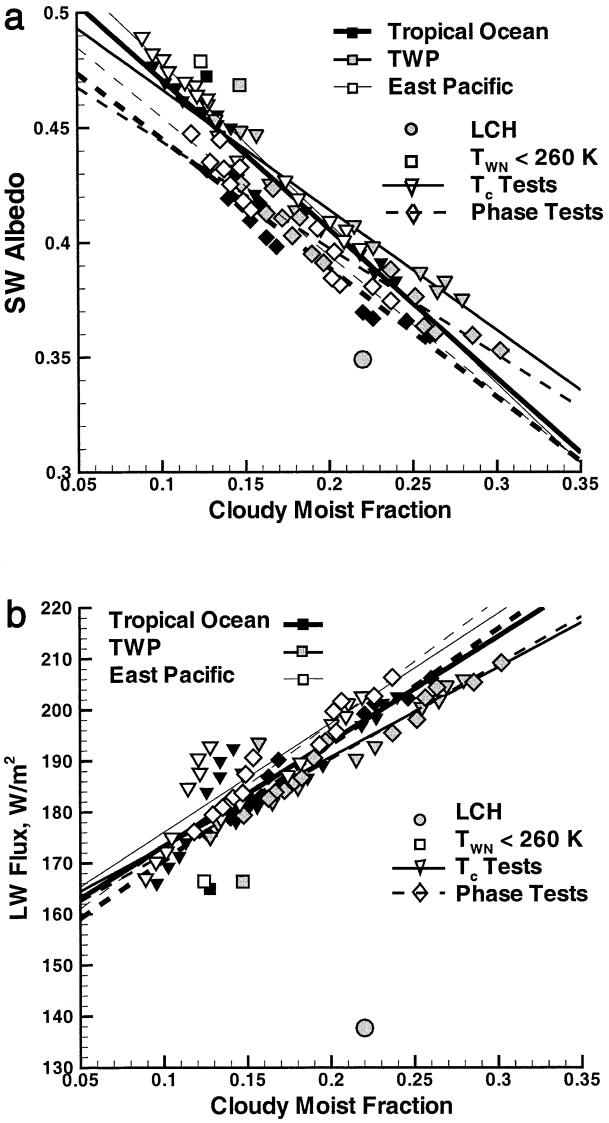


FIG. 1. (a) The SW albedo of the cloudy-moist region according to various definitions. The LCH value for the TWP region is shown by a circle. CERES values based strictly on $T_{WN}$ are shown by squares. Properties obtained using cloud temperature (triangles) or cloud phase (diamonds) tests are given for a variety of possible ways of defining the cloudy-moist region. (b) Same as (a) except for OLR.

Figure 2 shows the net flux into the cloudy-moist

[1] Combining TRMM microwave imager (TMI) data with VIRS cloud products, Ho et al. (2001) found that the mean cloud liquid water path (LWP) estimated from VIRS (which may include some thin cirrus) is only 0.005 mm different from that estimated by TMI (which only measures cloud water) when the Lin et al. (1998a,b) method is used. This suggests that if thin cirrus over water clouds were mislabeled as water clouds, the optical depth of the cirrus must be very small ($\tau < 0.25$). The effect on the radiative properties of the multilayer system, with a mean LWP of ~0.05 mm, should be less than 10%.

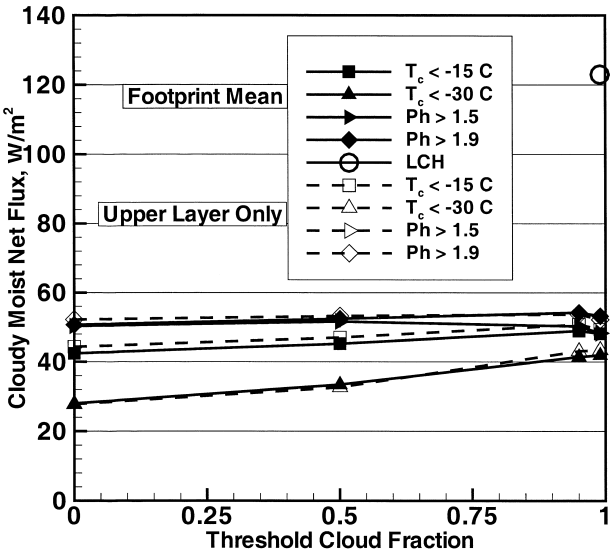


FIG. 2. Sensitivity of the net flux in the cloudy-moist region to the minimum amount of cloud cover within a CERES footprint, for various candidate definitions of that region.

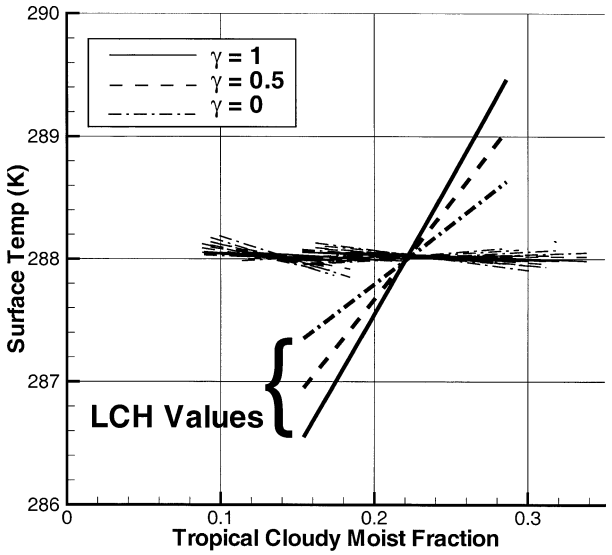


FIG. 3. Change in global average surface temperature as the fractional amount of tropical cloudy-moist area is changed. Thus, $\gamma = 1$ is the case where the clear-moist area changes as the cloudy-moist area, and $\gamma = 0$ is the case where the clear-moist area is unchanged. Heavy lines are from LCH. Thin lines use CERES TRMM SSF data to obtain the radiative properties under alternative definitions of the cloudy-moist region. The strong negative feedback of LCH changes to a much weaker positive or negative feedback, depending on the specific definition used for the cloudy-moist region.

region as a function of the threshold cloud fraction. The lowest net flux values result when CERES footprints containing only small amounts of very cold clouds are included. As the cloud fraction threshold is increased such that the cloud covers 95% or more of the CERES footprint, the net flux values all converge below 55 W m$^{-2}$. The differences between the various definitions and the sensitivity to the threshold cloud fraction are small. Other ways to define the cloudy-moist region using different thresholds for cloud phase, cloud temperature, and cloud fraction in a CERES footprint were also tried (not shown). In no case was a net flux near the LCH value of 123 W m$^{-2}$ found. The net flux for thin versus thick cirrus clouds was also examined. About 20% of the cirrus footprints have optical depth $\tau < 1$. The net flux for this thin cirrus alone is about 100 W m$^{-2}$, still lower than the LCH value.

## 5. Cloud feedback calculations

The radiative properties and area fractions from the CERES SSF analysis can be inserted in the simple climate model used by LCH. As in their study, the tropical cloudy-moist area is varied ±30%, as $A_{\text{cldm}} = A_{\text{cldm0}}(1 + \mu)$, where $\mu = -0.3$ to 0.3. Several possibilities are explored for the clear-moist area, $A_{\text{cm}} = A_{\text{cm0}}(1 + \gamma\mu)$. If $\gamma = 1$, its area follows the change in the cloudy-moist area. If $\gamma = 0$, the cloudy-moist area is fixed at its initial value, $A_{\text{cm0}}$. The global surface temperature (currently 288 K) response from a change in the cloudy-moist area fraction is shown in Fig. 3. The strong negative feedback found by LCH is reduced to a much weaker feedback. This feedback may be either slightly positive or slightly negative depending on which definition is used for the cloudy-moist region. In all cases, the feedback is much smaller than that found by LCH.

Table 2 summarizes the feedback from the 3.5-box model in terms of the slope of the lines in Fig. 3. This slope is defined such that a negative feedback has a negative value, and these are shown in bold in the table. To save space, not all cases are shown; however, for completeness, all cases resulting in a negative feedback are included in Table 2. The largest negative feedback effect found in this study, a decrease of 0.05 K for a 30% decrease in the tropical cloudy-moist fractions, occurs when $\gamma = 0$ with the phase-based definition of the cloudy-moist region (Table 2, case 30). In contrast, LCH found a −0.65-K change for the same change in the tropical cloudy-moist fraction. An even smaller negative feedback is found for several other phase-based definitions when $\gamma = 0$. A slight positive feedback is found in all remaining cases, except case 20, Table 2, where moderately cold clouds in the upper layer also produce a very small negative feedback. As noted in section 3, this result depends on the use of the correct averaging method to get both SW and LW cloud radiative properties. However, even when a simplistic averaging is applied, the results remain of the same order of magnitude. The largest positive feedback effect, an increase of 0.19 K for a 30% decrease in the tropical cloudy-moist fraction, occurs again with $\gamma = 0$ for case 21, Table 2 (CERES footprints with small amounts of very cold clouds in the upper cloud layer).

In contrast to the results of LCH, this study finds the

TABLE 2. Net flux and temperature feedback for alternate cloudy-moist definitions. Negative feedback is shown in bold.

| Case no. | Definition | $A_c$ threshold | Area coverage | Net flux (W m$^{-2}$) | $-dT/dA_c$ | | |
|---|---|---|---|---|---|---|---|
| | | | | | $\gamma = 1$ | $\gamma = 0.5$ | $\gamma = 0$ |
| LCH | LCH paper | 1.0 (assumed) | 0.22 | | **−22.0** | **−15.9** | **−9.82** |
| CERES footprint mean cloud properties | | | | | | | |
| 2 | $T_c < -15$°C | 0.5 | 0.219 | 45.2 | 0.82 | 0.99 | 1.17 |
| 4 | $T_c < -15$°C | 0.99 | 0.186 | 48.2 | 0.96 | 0.73 | 0.51 |
| 6 | $T_c < -30$°C | 0.5 | 0.126 | 33.4 | 1.42 | 2.35 | 3.29 |
| 8 | $T_c < -30$°C | 0.99 | 0.109 | 41.9 | 1.63 | 1.72 | 1.80 |
| 9 | Phase* > 1.5 | 0. | 0.260 | 50.3 | 0.69 | 0.27 | **−0.15** |
| 10 | Phase > 1.5 | 0.5 | 0.246 | 51.6 | 0.72 | 0.14 | **−0.45** |
| 12 | Phase > 1.5 | 0.99 | 0.145 | 48.3 | 1.23 | 0.90 | 0.57 |
| 14 | Phase > 1.9 | 0.5 | 0.163 | 52.4 | 1.10 | 0.4 | **−0.30** |
| 15 | Phase > 1.9 | 0.95 | 0.153 | 54.2 | 1.16 | 0.29 | **−0.60** |
| 16 | Phase > 1.9 | 0.99 | 0.148 | 53.2 | 1.20 | 0.41 | **−0.38** |
| Upper-layer cloud properties | | | | | | | |
| 18 | $T_c < -15$°C | 0.5 | 0.227 | 47.0 | 0.78 | 0.77 | 0.75 |
| 20 | $T_c < -15$°C | 0.99 | 0.143 | 49.4 | 0.31 | **−0.13** | **−0.58** |
| 21 | $T_c < -30$°C | 0. | 0.142 | 27.8 | 1.26 | 2.83 | 4.42 |
| 22 | $T_c < -30$°C | 0.5 | 0.134 | 32.7 | 1.33 | 2.39 | 3.46 |
| 24 | $T_c < -30$°C | 0.99 | 0.096 | 43.4 | 1.86 | 1.73 | 1.59 |
| 25 | Phase > 1.5 | 0. | 0.260 | 50.3 | 0.69 | 0.27 | **−0.15** |
| 26 | Phase > 1.5 | 0.5 | 0.246 | 51.7 | 0.72 | 0.14 | **−0.46** |
| 28 | Phase > 1.5 | 0.99 | 0.145 | 48.3 | 1.15 | 0.82 | 0.48 |
| 29 | Phase > 1.9 | 0. | 0.226 | 52.2 | 0.79 | 0.14 | **−0.52** |
| 30 | Phase > 1.9 | 0.5 | 0.220 | 53.2 | 0.81 | 0.04 | **−0.73** |
| 31 | Phase > 1.9 | 0.95 | 0.140 | 53.7 | 1.27 | 0.42 | **−0.43** |
| 32 | Phase > 1.9 | 0.99 | 0.127 | 52.2 | 1.40 | 0.66 | **−0.08** |

* Phase is defined on the SSF data product as 1 for pure water and 2 for pure ice.

largest effect when $\gamma = 0$ and the smallest effect when $\gamma = 1$ (the largest LCH feedback, −1.45 K, occurs when $\gamma = 1$). This follows from the very different properties of the dry region in the two approaches (Table 1). LCH assumed a small net flux input in the dry region relative to the moist region, so decreasing either cloudy-moist or clear-moist area coverage resulted in a very strong negative feedback. In contrast, the CERES measurements indicate that the net flux in the dry region is close to that of the moist region. As a result, decreasing the moist area has little effect.

The 3.5-box model is a simplified radiative energy balance model and mainly concerns the area coverage feedback of high clouds and their dynamically coupled moist and dry areas within the Tropics. This simple model may miss many feedbacks in the climate system, but it should provide a rough range of the climate variations if the physics of the Iris effect is correct. There is some question whether the change in cloudy-moist area with cloud-weighted SST actually represents a useful quantity (Hartmann and Michelsen 2002), and whether extrapolating it from a regional variation to a global response to warmer climate is appropriate. Regardless, the current results show that the proposed Iris hypothesis feedback is much weaker when objectively determined radiative properties are used in the model.

Other tropical feedbacks related to moisture and cloud, such as the temperature dependence of humidity associated with saturation vapor pressure, cloud water amount (or optical thickness), cloud height, and particle size and thermodynamic phase, are not considered. Most of these feedbacks are not even qualitatively well known: some of them may be positive, and some may be negative. For example, with a warmer atmosphere, saturation vapor pressure increases, and specific humidity purely caused by temperature should increase, which provides positive feedback. The uncertainty for this temperature-caused moisture feedback is dynamics, which could change the patterns of the moist and dry areas and the upper-tropospheric humidity. Since some ice or mixed phase clouds would change to water clouds with smaller particle sizes in a warmer climate, the clouds would have longer lifetimes and higher reflectivity than those in a cooler climate. A negative feedback is likely in this case. Because of its small net radiation and weak feedback, these missing moisture and cloud feedbacks may be equally or even more important than the Iris effect, which would enhance the conclusion (that there is no strong negative feedback from the Iris effect) of this study.

## 6. Conclusions

New data products are available from the Clouds and the Earth's Radiant Energy System (CERES) instrument, a part of the NASA Earth Observing System. The Single Scanner Footprint product combines radiative fluxes with extensive information on the cloud condi-

tions in the footprint, which are retrieved using the coorbiting imager instrument. These data have been analyzed to more accurately define the radiative properties for the various regions of the recently proposed adaptive infrared Iris hypothesis (Lindzen et al. 2001). A variety of ways of defining the cloudy-moist region were examined. Although the area covered is quite sensitive to the definition, the radiative properties of the cloudy-moist region were found to be quite insensitive to that definition. According to CERES, net radiation ranges between 42 and 51 W $m^{-2}$ for various portions of the proposed Iris climate model. This is in contrast to the values of 123 W $m^{-2}$ for cloudy moist, and 13 W $m^{-2}$ for the dry region, which were somewhat subjectively assigned by LCH. For alternate ways of defining the cloudy-moist region, net radiation values between 27 and 54 W $m^{-2}$ are found.

Using the CERES-measured radiative properties, the tropical cloud feedback is at most one-tenth of the maximum value hypothesized by LCH. In most of the cases considered, a small positive feedback is found. In the remaining cases a very small negative feedback is found. These results are basically consistent with previous studies using CERES ERBE-like data (Lin et al. 2002). They show that the tropical iris, if it exists, is much weaker than the one proposed by LCH. Thus, the CERES data do not support the existence of an effective IR iris.

*Acknowledgments.* The CERES data were obtained from the Atmospheric Sciences Data Center at the NASA Langley Research Center. Discussions with Bruce A. Wielicki on CERES data analysis were of great benefit. Erika Geier and Sandy Nolan provided invaluable assistance with the SSF data products. The comments of Ming-Dah Chou and an anonymous reviewer were valuable in improving the manuscript.

## REFERENCES

Barkstrom, B., E. Harrison, G. Smith, R. Green, J. Kibler, R. Cess, and the ERBE Science Team, 1989: Earth Radiation Budget Experiment (ERBE) archival and April 1985 results. *Bull. Amer. Meteor. Soc.,* **70,** 1254–1262.

Chambers, L. H., B. A. Wielicki, and N. G. Loeb, 2001: Shortwave flux from satellite-measured radiance: A theoretical study over marine boundary layer clouds. *J. Appl. Meteor.,* **40,** 2144–2162.

Chou, M. D., R. S. Lindzen, and A. Y. Hou, 2002: Comments on ''The iris hypothesis: A negative or positive cloud feedback?'' *J. Climate,* **15,** 2713–2715.

Fu, Q., M. Baker, and D. L. Hartmann, 2002: Tropical cirrus and water vapor: An effective earth infrared iris? *Atmos. Chem. Phys.,* **2,** 31–37.

Green, R. N., and B. A. Wielicki, 1995: Convolution of imager cloud properties with CERES footprint point spread function (Subsystem 4.4). Clouds and the Earth's Radiant Energy System (CERES) algorithm theoretical basis document, Vol. III: Cloud analyses and determination of improved top of atmosphere fluxes (Subsystem 4). NASA RP 1376, 242 pp. [Available online at http://asd-www.larc.nasa.gov/ATBD/ATBD.html.]

Hartmann, D. L., and M. L. Michelsen, 2002: No evidence for iris. *Bull. Amer. Meteor. Soc.,* **83,** 249–254.

Ho, S., B. Lin, and P. Minnis, 2001: Estimation of cloud properties over oceans using VIRS and TMI measurements on the TRMM satellite. Preprints, *Fifth Symp. on Integrated Observing Systems,* Albuquerque, NM, Amer. Meteor. Soc., 45–48.

Lin, B., P. Minnis, B. Wielicki, D. R. Doelling, R. Palikonda, D. F. Young, and T. Uttal, 1998a: Estimation of water cloud properties from satellite microwave and optical measurements in oceanic environments. II: Results. *J. Geophys. Res.,* **103,** 3887–3905.

——, B. Wielicki, P. Minnis, and W. B. Rossow, 1998b: Estimation of water cloud properties from satellite microwave and optical measurements in oceanic environments. I: Microwave brightness temperature simulations. *J. Geophys. Res.,* **103,** 3873–3886.

——, ——, L. H. Chambers, Y. Hu, and K.-M. Xu, 2002: The iris hypothesis: A negative or positive cloud feedback? *J. Climate,* **15,** 3–7.

Lindzen, R. S., M.-D. Chou, and A. Y. Hou, 2001: Does the earth have an adaptive infrared Iris? *Bull. Amer. Meteor. Soc.,* **82,** 417–432.

Loeb, N. G., N. Manalo-Smith, S. Kato, W. F. Miller, S. Gupta, P. Minnis, and B. A. Wielicki, 2003: Angular distribution models for top-of-atmosphere radiative flux estimation from the Clouds and the Earth's Radiant Energy System instrument on the Tropical Rainfall Measuring Mission Satellite. Part I: Methodology. *J. Appl. Meteor.,* in press.

Minnis, P., D. P. Garber, D. F. Young, R. F. Arduini, and Y. Takano, 1998: Parameterization of reflectance and effective emittance for satellite remote sensing of cloud properties. *J. Atmos. Sci.,* **55,** 3313–3339.

——, D. F. Young, B. A. Wielicki, P. W. Heck, X. Dong, L. L. Stowe, and R. Welch, 1999: CERES cloud properties derived from multispectral VIRS data. *Proc. SPIE,* **3867,** 91–102.

——, and Coauthors, cited 2002: Cloud optical property retrieval (Subsystem 4.3). Clouds and the Earth's Radiant Energy System (CERES) algorithm theoretical basis document. [Available online at http://asd-www.larc.nasa.gov/ATBD/ATBD.html.]

Priestley, K. J., and Coauthors, 2000: Postlaunch radiometric validation of the Clouds and the Earth's Radiant Energy System (CERES) Proto-Flight Model on the Tropical Rainfall Measuring Mission (TRMM) spacecraft through 1999. *J. Appl. Meteor.,* **39,** 2249–2258.

Rossow, W. B., A. W. Walker, and L. C. Garder, 1993: Comparison of ISCCP and other cloud amounts. *J. Climate,* **6,** 2394–2418.

Wielicki, B. A., R. D. Cess, M. D. King, D. A. Randall, and E. F. Harrison, 1995: Mission to Planet Earth: Role of clouds and radiation in climate. *Bull. Amer. Meteor. Soc.,* **76,** 2125–2153.

——, B. R. Barkstrom, E. F. Harrison, R. B. Lee III, G. L. Smith, and J. E. Cooper, 1996: Clouds and the Earth's Radiant Energy System (CERES): An Earth Observing System Experiment. *Bull. Amer. Meteor. Soc.,* **77,** 853–868.